Preoperative Detection of the *TERT* Promoter Mutations in Papillary Thyroid Carcinomas

Tomoe Nakao
Department of Endocrinology and Metabolism, Nagasaki University Graduate School of Biomedical Sciences
Michiko Matsuse (michikom@nagasaki-u.ac.jp)
Department of Radiation Medical Sciences, Atomic Bomb Disease Institute, Nagasaki University
Vladimir Saenko
Department of Radiation Molecular Epidemiology, Atomic Bomb Disease Institute, Nagasaki University.
Tatiana Rogounovitch
Department of Radiation Medical Sciences, Atomic Bomb Disease Institute, Nagasaki University
Aya Tanaka
Department of Surgical Oncology, Nagasaki University Graduate School of Biomedical Sciences
Keiji Suzuki
Department of Radiation Medical Sciences, Atomic Bomb Disease Institute, Nagasaki University
Miyoko Higuchi
Department of Diagnostic Pathology, Kuma Hospital
Hisanori Sasai
Department of Otorhinolaryngology, Kuma Hospital
Tsutomu Sano
Department of Otorhinolaryngology, Kuma Hospital
Mitsuyoshi Hirokawa
Department of Diagnostic Pathology, Kuma Hospital
Akira Miyauchi
Department of Surgery, Kuma Hospital
Atsushi Kawakami
Department of Immunology and Rheumatology, Nagasaki University Graduate School of Biomedical Sciences
Norisato Mitsutake
Department of Radiation Medical Sciences, Atomic Bomb Disease Institute, Nagasaki University

Research Article

Keywords: TERT promoter mutation, BRAFV600E mutation, fine needle aspiration, molecular marker, papillary thyroid carcinoma

Posted Date: February 24th, 2021

DOI: https://doi.org/10.21203/rs.3.rs-228278/v1

Version of Record: A version of this preprint was published at Clinical Endocrinology on July 28th, 2021. See the published version at https://doi.org/10.1111/cen.14567.

Abstract

Telomerase reverse transcriptase promoter (*TERT*-p) mutations are strongly associated with tumor aggressiveness and worse prognosis in papillary thyroid carcinomas (PTCs). Since the *TERT*-p promoter mutations have been reported to be subclonal, it is unclear how accurately they can be detected by preoperative fine needle aspiration (FNA). The objective of this study was to analyze the concordance rate of the *TERT*-p mutations between preoperative FNA and corresponding postoperative surgical specimens. The mutational status of the *TERT*-p in FNA samples detected by our ddPCR assay was highly concordant with that in postoperative FFPE specimens. The *TERT*-p mutation was significantly associated with age, tumor size, extrathyroidal extension, and the Ki-67 labeling index in multivariate analysis in both FNA and FFPE samples. The detection of the *TERT*-p mutations using FNA samples has a good ability to predict disease aggressiveness and, therefore, could be clinically useful in the determination of PTC management.

Introduction

The incidence of thyroid cancers has increased in recent years. This increase is mostly attributed to papillary thyroid carcinomas (PTCs) [1]. Although PTCs usually have a favorable prognosis, 10–15% of patients have recurrences, some of which become refractory to treatments [2,3].

The $BRAF^{V600E}$ mutation is the most common genetic alteration in PTCs. Its prevalence varies from 30–80% [4], which seems to be dependent on the study population. Many studies have reported an association between the presence of the $BRAF^{V600E}$ mutation and aggressive clinicopathological features in PTCs [5–7]. On the other hand, there are also studies, especially from Japan, demonstrating no such relationship [8,9]. Thus, the clinicopathological significance of $BRAF^{V600E}$ is not universal and still remains controversial.

Two somatic mutations, located − 124 and − 146 base pairs upstream from the ATG start site (− 124C > T and − 146C > T) of the telomerase reverse transcriptase (*TERT*) gene have been found in PTCs [10,11]. They are mutually exclusive, and the average frequency of either mutation in PTCs has been reported to be about 10% [12], which seems to have no major difference between populations. The *TERT* promoter (*TERT*-p) mutations strongly correlate with older patient age [9,13–19]. Many studies have consistently demonstrated that the coexistence of the $BRAF^{V600E}$ mutation and the *TERT*-p mutation is strongly associated with aggressive clinicopathological characteristics and worse prognosis [9,14,16,20–26]. So far, the *TERT*-p mutations are the best prognostic molecular marker in PTCs. Therefore, their preoperative detection in fine-needle aspiration (FNA) specimens could be useful in the determination of PTC management.

The *TERT*-p mutations have been reported to be an early event during cancer progression in glioblastoma, hepatocellular carcinoma, and melanoma, whereas in thyroid cancer, they have been reported to be a late

event [27,28]. If the *TERT*-p mutations are a late event, only a fraction of cancer cells harbor the mutation, and the frequency of the mutant allele is supposed to be low. Indeed, according to The Cancer Genome Atlas (TCGA) data, the allele frequencies of the *TERT*-p mutations were 5–50% (23% on average) [29], suggesting that the *TERT*-p mutations are not a clonal event in many PTCs. Based on these findings, it is unclear whether preoperative FNA can be effectively used to detect the *TERT*-p mutations.

There are four studies that preoperatively analyzed the *TERT*-p mutations using FNA or core-needle biopsy (CNB) samples in thyroid carcinomas [22,30–32]. These studies evaluated the *TERT*-p mutations in only preoperative FNA or CNB specimens, but comparison with postoperative surgical tissues was not performed. Considering that the *TERT*-p mutations are not always clonal in PTCs, it is not clear how accurately the *TERT*-p mutations could be detected in preoperative FNA samples. In this study, therefore, we analyzed the concordance rate of the *TERT*-p mutations between FNA and surgical specimens.

Material And Methods

PTC samples and patient information

Between August 2017 and July 2019, 96 PTC patients aged 55 years or older (range: 55–81, median: 67.0, interquartile range: 71.8–59.0, 19.8% male) were recruited at Kuma Hospital (Kobe, Japan) because the *TERT*-p mutations are rare under the above age. Clinicopathological data were collected from the patients' medical records. Median nodule size was 16.0 mm (range: 6–110, interquartile range: 23.0–11.0). Their histological subtypes were: 85 classic PTCs, 1 follicular variant of PTC, 7 tall cell variants of PTCs, 2 hobnail variant of PTCs and 1 Warthin-like variant of PTC. The study protocol was approved by the institutional review boards of Nagasaki University and Kuma Hospital. Written informed consent was obtained from each patient. All methods were carried out in accordance with the relative guidelines and regulations.

Ultrasound-guided FNA was performed by well-experienced operators using a 22-gauge needle fitted to a 10 mL syringe. Most of the material from the needle was used for cytological examination, and the remaining was used for DNA extraction by washing needles with 1 mL of RNA later (Thermo Fisher Scientific). All samples were stored at 4℃ for up to one month. DNA were extracted using ISOGEN reagent (Nippon Gene). The corresponding postoperative formalin-fixed and paraffin-embedded (FFPE) specimens were obtained, and DNA was extracted from manually microdissected tumor portions using a QIAamp DNA mini kit (QIAGEN). For each case, we used 1–4 serial sections of 10 μm thickness, depending on the tumor size.

Droplet digital PCR for the TERT promoter and BRAF^{V600E} mutations

Droplet digital PCR (ddPCR) to detect the *TERT*-p mutations was performed as previously described [19]. Uracil-DNA Glycosylase (Invitrogen) treatment was used in ddPCR in both FNA and FFPE samples. To

detect the *BRAF*^{V600E} mutation by ddPCR, primer sequences were: *BRAF* F 5'-ACTACACCTCAGATATATTTCTTCATGA-3' and *BRAF* R 5'-AGCCTCAATTCTTACCATCCACA-3; probes: *BRAF* mut, 5'-/5HEX/CT + ACA + G + A + GA + AA + TCT/3IABkFQ/-3' and *BRAF* wt 5'-/56-FAM/CT + ACA + G + T + GA + AA + TCT/3IABkFQ/-3' (a base preceded by + is Locked Nucleic Acid).

Statistical analysis

QuantaSoft software (Bio-Rad Laboratories) was used to determine the copy number data and other relevant information from ddPCR runs. The Fisher's exact test or Fisher-Freeman-Halton exact test was used for categorical data, and the Mann-Whitney test was used for continuous data to compare between any two (sub)groups. Multivariable linear, logistic, or ordinal response regression models were used to analyze the associations between the *TERT*-p status and clinicopathological parameters. Logistic regression models with very small numbers of outcomes (< 5 per cell) were conducted using Firth's approach to bias-reducing penalized maximum likelihood fit using the LOGISTIC procedure in the 9.4M5 version of SAS (SAS Institute). Multivariable linear and ordinal response models were run using the GENMOD procedure using appropriate distributions and link functions. All *p*-values were two-sided and considered significant if $p < 0.05$.

Results

Establishment of the ddPCR assay

Our ddPCR assay specifically detected the wild-type and mutant alleles of the *TERT*-p and *BRAF* (Fig. 1). To evaluate the quantitative performance of the assay, serially diluted mutant PCR products were mixed in wild-type PCR products to obtain various reference samples with mutation fractions of 0, 1, 5, 10, 50, and 100%. For each, four different sets of total DNA copies of 500, 1,000, 3,000 and 9,000 were prepared and analyzed. The expected and observed mut% were well correlated in all tested samples of both genes, and all coefficients of determination were > 0.989 (Supplementary Fig. S1).

Since the *TERT*-p mutations are C > T transitions, artificial C > T mutations during PCR caused by hydrolytic deamination of cytosine are a problem in precise detection of the *TERT*-p mutations, especially in stored DNAs. The cytosine deamination creates uracil, and uracil can pair with adenine during elongation, leading to the C > T mutation and causing a false positive. We used uracil DNA glycosylase to avoid the false positive; however, it was not possible to completely eliminate it. Therefore, the cutoff limit for detection of the *TERT*-p mutation in the ddPCR assay was statistically determined by analyzing serially diluted mutant PCR products mixed with wild-type PCR products and 100% wild-type PCR products. We determined mut% that yielded the number of mutant signals significantly exceeding the background, calculated the 95% prediction interval for those values, and used its upper boundary as the cutoff; all samples displaying *TERT*-p mut% above the cutoff were considered *TERT*-p mutation-positive. See Supplementary file 1 with Supplementary Fig. S2 for detailed calculations.

In addition, we determined the minimal DNA copy number in a reaction that was necessary to correctly distinguish the true negative samples from those showing no *TERT*-p mutant signals due to insufficient amount of template DNA. Under the conditions used in our ddPCR, the minimal number of *TERT*-p DNA copies in a reaction was more than 64 (Supplementary file 1). Samples with the total *TERT*-p DNA copy number ≤ 64 were considered “inadequate”.

Analysis of FNA and FFPE samples by the ddPCR

A total of 96 nodules with pathologically confirmed PTC were analyzed. Based on the cutoff limits, 19 (20%) and 4 (4%) of the FNA samples were found to carry the − 124C > T and − 146C > T mutations, respectively, 66 (69%) were wild-type, and 7 (7%) were inadequate (Fig. 2a). Of the corresponding 96 FFPE samples, 24 (25%) and 4 (4%) had the − 124C > T and − 146C > T mutations, respectively, and 68 (71%) were wild-type (Fig. 2b). All FFPE samples were successfully genotyped (Fig. 2b). Results of the *TERT*-p mutation analysis in FNA and FFPE samples are summarized in Fig. 3a and b, respectively. Assuming FFPE result a true condition and that of FNA a predicted condition, the area under curve in receiver operating characteristic analysis (AUC-ROC) was 0.899 (95% CI: 0.810–0.989). The sensitivity, specificity, positive predictive value (PPV), and negative predictive value (NPV) were 81.5, 98.4, 95.7, and 92.4%, respectively (Fig. 3c). The Cohen’s kappa was 0.834 (p = 2.52E-15), which corresponds to “almost perfect agreement” [33]. A total of 6 cases had discordant results: 1 case was FNA mut/FFPE wt and 5 cases were FNA wt/FFPE mut.

The $BRAF^{V600E}$ mutation was also examined by the same fashion. The $BRAF^{V600E}$ mutation is a T > A transversion, and we did not observe any false positive in our ddPCR assay. Of the 96 FNA samples, 85 (89%) were found to carry the $BRAF^{V600E}$ mutation and 7 (7%) were wild-type (Fig. 3d). There were four (4%) inadequate cases (Fig. 3d). Of the 96 corresponding FFPE samples, 91 (95%) had the $BRAF^{V600E}$ mutation and 5 (5%) wild-type (Fig. 3e). All FFPE samples were successfully genotyped. The AUC-ROC was 0.888 (95% CI: 0.679–1.000), and the sensitivity, specificity, PPV, and NPV were 96.6, 80.0, 98.8 and 57.1%, respectively (Fig. 3f). The Cohen’s kappa was 0.710 (p = 1.02E-11), corresponding to “substantial agreement” [33]. A total of 4 cases displayed discordant results: 1 case was FNA mut/FFPE wt and 3 cases were FNA wt/FFPE mut. In our series, all *TERT*-p mutation-positive samples harbored the $BRAF^{V600E}$ mutation in both the FNA and FFPE samples.

Relationship Between The Mutational Status And Clinicopathological Features

First, we analyzed the relationship between the mutational status of the *TERT*-p in FFPE samples and clinicopathological features. The median ages of patients with mutation-positive and wild-type PTCs were 71.5 (interquartile range: 74.8–67.5) and 64.5 (69.0–58.0) years old, respectively, and this difference was significant in both univariate (p = 1.68E-05) and multivariate (p = 5.00E-06) analysis (Table 1). The median tumor size was significantly greater in the mutation-positive cases (20.5, 27.5–16.0 mm) than in

the wild-type cases (13.0, 20.0–10.0 mm) in both univariate (p = 0.002) and multivariate (p = 0.032) analysis. (Table 1). The advanced AJCC 8th edition's pT categories were more frequently observed in the *TERT*-p mutation-positive PTCs (multivariate p = 0.015) (Table 1). The mutation-positive tumors displayed a significantly higher risk for extrathyroidal extension than wild-type ones (multivariate p = 0.015). The Ki-67 labeling index in the *TERT*-p mutation-positive tumors was significantly higher than that in the wild-type in both univariate (p = 6.41E-10) and multivariate (p = 2.00E-06) analysis (Table 1).

Table 1

Association between the *TERT*-p mutational status and clinicopathological features in FFPE samples. Multivariate: Adjusted for age, sex and *BRAF* status. Abbreviations: CI, confidence interval; IQR, interquartile range; nc, not calculated; nd, not determined; LN, lymph node. Statistical test: [a]Mann-Whitney test. [b]Linear regression model. [c]Fisher exact test. [d]Fisher–Freeman–Halton exact test. [e]Ordinal response model.

		Univariate			**Multivariate**	
Parameter	All FFPE cases	*TERT* mut-	*TERT* mut+	*p*	β or OR (95% CI)	*p*
Number of cases	96	68	28			
Age (years old) median (IQR, Q3-Q1)	67.0 (71.8–59.0)	**64.5 (69.0–58.0)**	**71.5 (74.8–67.5)**	**1.68E-05**[a]	**6.485 (3.699-9.271)**[b]	**5.00E-06**
(range)	(55-81)	(55-80)	(56-81)			
Sex F/M, ratio	77/19 (4.1:1)	55/13 (4.2:1)	22/6 (4.1:1)	0.784[c]	0.487 (0.137-1.733)	0.267
Tumor size (mm) median (IQR, Q3-Q1)	16.0 (11.0, 23.0)	**13.0 (20.0–10.0)**	**20.5 (27.5–16.0)**	**0.002**[a]	**6.797 (0.589-13.005)**[b]	**0.032**
(range)	(6-110)	(6-110)	(9-43)			
pT3&4 *vs* pT1&2 (7th)	92 (96.8%)	66 (98.5%)	26 (92.9%)	0.207[c]	0.169 (0.018-1.542)	0.115
pT3&4 *vs* pT1&2 (8th)	12 (12.5%)	6 (8.8%)	6 (21.4%)	0.102[c]	**7.543 (1.489-38.214)**	**0.015**
pN	63 (65.6%)	42 (61.8%)	21 (75.0%)	0.400[c]	1.568 (0.411-5.984)	0.511
M	2 (2.1%)	1 (1.5%)	1 (3.7%)	0.490[c]	2.914 (0.142-59.712)	0.488

		Univariate			Multivariate	
Extrathyroidal extension (gross)	6 (6.3%)	2 (2.9%)	4 (14.3%)	0.058[c]	**12.517 (1.628-96.223)**	**0.015**
Stage (7th)				0.129[d]	**1.155 (0.009-2.301)[e]**	**0.048**
Not determined	15 (15.6%)	12 (17.6%)	3 (10.7%)	nc	nc	nc
I	0	0	0	nd	nd	nd
II	0	0	0	nd	nd	nd
III	53 (65.4%)	40 (71.4%)	13 (52.0%)	0.129[c]	**0.315 (0.100-0.991)**	**0.048**
IV	28 (34.6%)	16 (28.6%)	12 (48.0%)	0.129[c]	**3.174 (1.009-9.980)**	**0.048**
Stage (8th)				0.263[d]	1.013 (-0.019-2.045)[e]	0.054
Not determined	1 (1.0%)	0	1 (3.6%)	nc	nc	nc
I	31 (32.3%)	25 (36.8%)	6 (22.2%)	0.227[c]	0.429 (0.138-1.332)	0.143
II	56 (58.3%)	39 (57.4%)	17 (63.0%)	0.651[c]	1.236 (0.447-3.416)	0.683
III	6 (6.3%)	3 (4.4%)	3 (11.1%)	0.347[c]	6.687 (0.923-48.311)	0.060
IV	2 (2.1%)	1 (1.5%)	1 (3.7%)	0.490[c]	2.914 (0.142-59.712)	0.488

		Univariate			Multivariate	
Total thyroidectomy	70 (72.9%)	47 (69.1%)	23 (82.1%)	0.218[c]	2.223 (0.669-7.384)	0.192
LN dissection (more than central)	25 (26.0%)	15 (22.1%)	10 (35.7%)	0.203[c]	2.895 (0.928-9.030)	0.067
Ki-67 labeling index				**6.41E-10**[d]	**3.159 (1.867-4.451)**[e]	**2.00E-06**
0–5%	**70 (72.9%)**	**62 (91.2%)**	**8 (28.6%)**	**1.72E-09**[c]	**0.045 (0.012-0.166)**	**3.00E-06**
5–10%	**20 (20.8%)**	**6 (8.8%)**	**14 (50.0%)**	**2.20E-05**[c]	**11.093 (3.011-40.973)**	**2.99E-04**
> 10%	**6 (6.3%)**	**0**	**6 (21.4%)**	**4.06E-04**[c]	**23.124 (1.306-409.375)**	**0.032**
FFPE *BRAF*^{V600E} mutation	91 (94.8%)	63 (92.6%)	28 (100%)	0.317[c]	4.018 (0.194-83.221)	0.368

Next, we analyzed the clinicopathological correlations with the *TERT*-p mutation in FNA samples. The median ages of patients with mutation-positive and wild-type PTCs were 71.5 (74.3–67.0) and 65.5 (69.0-58.3) years old, respectively; the difference was significant in both univariate (p = 5.61E-04) and multivariate (p = 4.53E-04) analysis (Table 2). The median tumor size was significantly greater in the mutation-positive cases (22.0, 28.3–14.0 mm) than in the wild-type cases (13.0, 20.8–10.3 mm) in univariate analysis (p = 0.011) (Table 2). In multivariate analysis, this significance was lost, although the effect size was still high (b = 6.732, p = 0.056) (Table 2). The advanced AJCC 8th edition's pT categories were more frequently observed in the *TERT*-p mutation-positive PTCs (multivariate p = 0.05) (Table 2). Extrathyroidal extension was more common in the mutation-positive cases than in the wild-type cases (univariate p = 0.035 and multivariate p = 0.009) (Table 2). The Ki-67 labeling index in the mutation-positive PTCs was significantly higher than in the wild-type tumors in both univariate (p = 3.46E-05) and multivariate analyses (p = 0.002) (Table. 2).

Table 2

Association between the *TERT*-p mutational status and clinicopathological features in FNA samples. Multivariate: Adjusted for age, sex and *BRAF* status. Abbreviations: CI, confidence interval; IQR, interquartile range; nc, not calculated; nd, not determined; LN, lymph node. Statistical test: [a]Mann-Whitney test. [b]Linear regression model. [c]Fisher exact test. [d]Fisher–Freeman–Halton exact test. [e]Ordinal response model.

		Univariate			**Multivariate**	
Parameter	All FNA cases	*TERT* mut-	*TERT* mut+	*p*	β or OR (95% CI)	*p*
Number of cases	86	64	22			
Age, median (years old) (IQR, Q3-Q1)	67.0 (72.0–59.0)	**65.5 (69.0-58.3)**	**71.5 (74.3–67.0)**	**5.61E-04**[a]	**5.469 (2.412–8.525)**[b]	**4.53E-04**
(range)	(55–81)	(55–81)	(56–77)			
Sex F/M, ratio	69/17 (4.1:1)	53/11 (4.8:1)	16/6 (2.7:1)	0.356[c]	**0.244 (0.060–0.986)**	**0.048**
Tumor size, median (mm) (IQR, Q3-Q1)	15.5 (23.3–11.0)	**13.0 (20.8–10.3)**	**22.0 (28.3–14.0)**	**0.011**[a]	6.732 (-0.165–13.626)[b]	0.056
(range)	(6–110)	(6–110)	(9–43)			
pT3&4 *vs* pT1&2 (7th)	84 (97.7%)	64 (100%)	20 (90.9%)	0.063[c]	0.060 (0.003–1.199)	0.066
pT3&4 *vs* pT1&2 (8th)	12 (14.0%)	6 (9.4%)	6 (27.3%)	0.068[c]	**14.138 (2.231–89.613)**	**0.005**
pN	55 (64.0%)	39 (60.9%)	16 (72.7%)	0.441[c]	1.256 (0.280–5.640)	0.766
M	1 (1.2%)	1 (1.6%)	0	1.000[c]	0.910 (0.043–19.496)	0.952

		Univariate			Multivariate	
Extrathyroidal extension (gross)	6 (7.0%)	**2 (3.1%)**	**4 (18.2%)**	**0.035**[c]	**24.586 (2.229–271.212)**	**0.009**
Stage (7th)				0.261[d]	0.829 (-0.358–2.016)[e]	0.171
Not determined	14 (16.3%)	11 (17.2%)	3 (13.6%)	nc	nc	nc
I	0	0	0	nd	nd	nd
II	0	0	0	nd	nd	nd
III	47 (54.7%)	37 (57.8%)	10 (45.5%)	0.261[c]	0.436 (0.133–1.431)	0.171
IV	25 (29.1%)	16 (25.0%)	9 (40.9%)	0.261[c]	2.291 (0.699–7.510)	0.171
Stage (8th)				0.332[d]	0.847 (-0.255–1.950)[e]	0.132
Not determined	1 (1.2%)	0	1 (4.5%)	nc	nc	nc
I	29 (33.7%)	24 (37.5%)	5 (22.7%)	0.298[c]	0.546 (0.163–1.828)	0.326
II	49 (57.0%)	36 (56.3%)	13 (59.1%)	0.8[c]	0.943 (0.309–2.880)	0.918
III	6 (7.0%)	3 (4.7%)	3 (13.6%)	0.157[c]	**12.680 (1.240–129.713)**	**0.032**
IV	1 (1.2%)	1 (1.6%)	0	1.000[c]	0.676 (0.033–13.716)	0.799

		Univariate			Multivariate	
Total thyroidectomy	60 (69.8%)	41 (64.1%)	19 (86.4%)	0.062[c]	3.969 (0.977–16.129)	0.054
LN dissection (more than central)	22 (25.6%)	15 (23.4%)	7 (31.8%)	0.572[c]	1.611 (0.486–5.336)	0.435
Ki-67 labeling index				**3.46E-05**[d]	**1.825 (0.680–2.970)**[e]	**0.002**
0–5%	62 (72.1%)	**54 (84.4%)**	**8 (36.4%)**	**4.30E-05**[c]	**0.107 (0.033–0.343)**	**1.74E-04**
5–10%	19 (22.1%)	**9 (14.1%)**	**10 (45.5%)**	**0.006**[c]	**5.868 (1.780–19.346)**	**0.004**
> 10%	5 (5.8%)	**1 (1.6%)**	**4 (18.2%)**	**0.014**[c]	**12.244 (1.184–126.591)**	**0.036**
FNA *BRAF*^{V600E} mutation	80 (93.0%)	58 (90.6%)	22 (100%)	0.331[c]	2.293 (0.119–44.335)	0.583

Correspondence analysis demonstrated that the mutational status of *TERT*-p and *BRAF* determined by FNA and that by FFPE were highly correlated. Other parameters showing high correlation with the mutational status were higher Ki-67 labeling index and age > 69 years old (Supplementary Fig. S3).

The clonality of the TERT promoter mutation

The allelic frequency of the *TERT*-p mutation does not accurately tell us the clonality of the *TERT*-p mutation in cancer cells because tumor tissue contains not only tumor cells but also stromal, endothelial, and blood cells. Therefore, we used the allelic frequency of the *BRAF*^{V600E} mutation as an indicator of tumor purity since the *BRAF*^{V600E} mutation has been reported to be a clonal event in PTCs [28,34], and our immunohistochemical staining using specific antibody for BRAF^{V600E} also demonstrated homogeneous staining in PTC cells in the FFPE specimens (data not shown).

We calculated the proportion of the *TERT*-p mutation-positive cancer cells (TP) by dividing the allelic frequency of the *TERT*-p mutation by that of the *BRAF*^{V600E} mutation. In the 28 FFPE samples that

harbored the *TERT*-p mutation, the TPs varied from 51–136% (Fig. 4), although in most cases they were 80–120%, suggesting that the *TERT*-p mutation may be nearly clonal in most PTCs. Two cases had higher TPs (135.0% and 135.5%), and three cases had lower TPs (51.1, 52.8 and 65.7%) (Fig. 4), which could be due to copy gain and low clonality, respectively. We also analyzed the association of the TP with clinicopathological characteristics. As shown in Table 3, the higher TP was significantly associated with the higher pT category of both the 7th (multivariate $p = 0.023$) and 8th (multivariate $p = 0.005$) editions of AJCC TNM classification and extrathyroidal extension (univariate $p = 0.015$ and multivariate $p = 0.05$).

Table 3

Linear association between the proportion of *TERT*-p positive cancer cells and clinicopathological features in FFPE samples. Multivariate: Adjusted for age and sex. Abbreviations: CI, confidence interval; nd, not determined. Statistical test: [a] Pearson correlation coefficient. [b] Linear regression model. [c] Mann-Whitney test. [d] Kruskal-Wallis test. [e] Ordinal response model. [f] Kruskal-Wallis test with Dunn's post hoc test.

	proportion of *TERT*-p positive cancer cells	**Univariate**	**Multivariate**	
Parameter	Regression coefficient (95% CI)	*p*	β or OR (95% CI)	*p*
Age	0.633 (-0.483–1.749)[a]	0.254	0.067 (-0.037–0.171)[b]	0.210
Sex		0.236[c]	1.025 (0.976–1.076)	0.329
M	0.862 (0.828–0.871)			
F	0.950 (0.823–1.066)			
Tumor size	0.461 (-0.124–1.046)[a]	0.303	0.117 (-0.048–0.283)[b]	0.164
pT (7th)		0.059[d]	**1.070 (1.010–1.134)**[e]	**0.023**
1	nd	nd	nd	nd
2	0.849 (0.657–1.040)	0.640[f]	0.982 (0.927–1.041)	0.544
3	0.875 (0.823–0.977)	0.100[f]	0.969 (0.922–1.019)	0.223
4	1.100 (1.045–1.251)	**0.015**[f]	**1.105 (1.000–1.222)**	**0.05**
3&4 *vs* 1&2	0.886 (0.828–1.052)	0.640[c]	1.018 (0.961–1.078)	0.544
pT (8th)		**0.028**[d]	**1.075 (1.023–1.129)**[e]	**0.005**
1	0.828 (0.800–0.910)	0.013[f]	0.944 (0.890–1.002)	0.059
2	0.891 (0.859–1.043)	0.746[f]	0.982 (0.942–1.025)	0.411
3	1.052 (0.960–1.201)	0.248[f]	1.093 (0.979–1.220)	0.112
4	1.147 (1.088-–.251)	**0.032**[f]	1.190 (0.986–1.435)	0.069

	proportion of *TERT*-p positive cancer cells	Univariate	Multivariate	
2&3&4 *vs* 1	1.029 (0.878–1.066)	**0.013**[c]	1.059 (0.998–1.123)	0.059
3&4 *vs* 1&2	1.100 (1.029–1.350)	**0.010**[c]	**1.221 (1.008–1.479)**	**0.041**
pN	-0.463 (-20.788–19.862)	0.963[c]	0.984 (0.920–1.052)	0.629
M	0.915 (0.828–1.052)	0.444[c]	0.996 (0.938–1.057)	0.883
Extrathyroidal extension (gross)	1.100 (1.041–1.251)	**0.015**[c]	**1.105 (1.000–1.222)**	**0.050**
Stage (7th)		0.052[d]	1.071 (0.999–1.149)[e]	0.054
Stage (8th)		0.159[d]	1.025(0.984–1.068)[e]	0.240
Ki-67 labeling index		0.390[d]	1.032 (0.991–1.075)[e]	0.129
0–5%	0.850 (0.676–0.990)	0.182[f]	0.976 (0.932–1.021)	0.288
5–10%	0.920 (0.857–1.052)	0.401[f]	1.001 (0.962–1.042)	0.951
> 10%	0.920 (0.840–1.119)	0.682[f]	1.045 (0.975–1.119)	0.216

Discussion

In this study, we analyzed the concordance rate of the *TERT*-p mutations between preoperative FNA specimens and their postoperative counterparts using a highly sensitive ddPCR technique. There have been three studies that preoperatively analyzed the *TERT*-p mutations using FNA samples in thyroid carcinomas [22,30,31]. According to these reports, the frequency of the mutations ranged from 4.5 to 14.5%, but none of these studies assessed the performance of analyzing the mutations using FNA by comparing with surgical specimens. Our present study is the first report to evaluate the concordance rate of the *TERT*-p mutations between preoperative FNA specimens and their postoperative counterparts.

In the present study, the frequencies of the *TERT*-p mutations in FNA and FFPE samples were 24% and 29%, respectively, which was higher than in previous reports. One of the reasons is that we recruited PTC patients aged 55 years or older since the *TERT*-p mutations have been reported to correlate with older

patient age [13–18]. Another reason for the higher frequency of the *TERT*-p mutations may be the use of ddPCR assay, which is more sensitive than conventional Sanger sequencing and real-time PCR.

The *TERT*-p mutations were significantly associated with age, tumor size, extrathyroidal extension, and the Ki-67 labeling index in not only the results obtained from the FFPE sections but also those from the FNA samples. Therefore, the mutational status of the *TERT*-p analyzed using preoperative FNA samples can be used as a predictive marker for disease aggressiveness and prognosis. This analysis may enable us to select an optimal strategy, such as applying total thyroidectomy from the first operation even with a small PTC with no nodal metastasis.

The sensitivity of the *TERT*-p mutations in FNA specimens was 81.5%. We had expected that the detection rate of the *TERT*-p mutations in FNA specimens could have been lower because the TCGA data showed that the mutant allele frequencies of the *TERT*-p mutations were 5–50% (23% on average) [29]. They used driver oncogenes to calculate tumor purity to exclude normal alleles from non-tumor cells, which is a basically same method as ours. In this study, we calculated the TP using the allelic frequency of the $BRAF^{V600E}$ mutation to adjust for tumor purity. The mean TPs were 80–120% in most of the cases, suggesting that the *TERT*-p mutations are a nearly clonal event in many PTCs. We do not have a good explanation about this discrepancy between the TCGA data and our present results. We had two cases with higher TP (135.0% and 135.5%), and gene amplification may be involved in these cases. On the other hand, there were three cases with lower TP (51.1, 52.8, and 65.7%), and in these cases, the *TERT*-p mutations were considered to be subclonal. We also found the significant association of the TP value with higher pT and extrathyroidal extension, suggesting that the TP may be correlated with aggressive properties.

In some cases, the mutational status was not consistent between FNA and FFPE samples. All five FNA specimens that were FNA wt/FFPE mut for the *TERT*-p mutation had sufficient amounts of DNA (see Fig. 2a), and their TPs were not low (78.8%, 84.0%, 86.7%, 94.9% and 135%). For the $BRAF^{V600E}$ mutation, there were three FNA wt/FFPE mut cases. One possible explanation for the results is the absence of mutation-positive cells in the solution obtained by washing needles. If so, it might be possible to increase the sensitivity by using the whole contents in the needle. The frequency of the *TERT*-p mutation in one FNA specimen (FNA mut/FFPE wt) was just above the cutoff value. Cases that are close to the cutoff value should be judged carefully, and, if possible, retesting is recommended.

There are some limitations of this study. First, the confusion matrix was composed assuming that the results of the *TERT*-p mutations in the FFPE samples were true. However, one can imagine that the FFPE sections may not represent a whole tumor. Second, due to the short observation period, we were not able to examine the association between the mutational status and the risk of recurrence.

In summary, the mutational status of the *TERT*-p in the FNA samples detected by our ddPCR assay was highly concordant with that in the postoperative FFPE sections. Our test method had high sensitivity and specificity, and the results were significantly associated with conventional clinicopathological parameters

correlated with disease aggressiveness. Therefore, preoperative detection of the *TERT*-p mutations in FNA specimens could be clinically useful in the determination of PTC management.

Declarations

Acknowledgements

The authors sincerely thank the financial support from the Japan Society for the Promotion of Science (JSPS KAKENHI) Grant Numbers 19K09913. The authors also thank all the participants who took part in this study.

Author Contributions

TN, MM, and TR performed experiments. TN, MM, and VS analyzed the data. TN, MM, VS, and NM contributed to experimental strategy and interpretation of the data and wrote the manuscript. MM raised funds. VS performed the statistical analysis. M Higuchi, HS, TS, M Hirokawa, and AM contributed to sample collection and clinical data acquisition. M Hirokawa performed pathological diagnosis. AT, KS and AK helped for data interpretation. MM and NM conceived and designed the study. All authors read and approved the final manuscript.

Competing interests

The authors declare no competing interests.

Data availability

The datasets generated during the current study are available upon reasonable request.

References

1. Wiltshire, J. J., Drake, T. M., Uttley, L. & Balasubramanian, S. P. Systematic Review of Trends in the Incidence Rates of Thyroid Cancer. *Thyroid.* **26**, 1541–1552 https://doi.org/10.1089/thy.2016.0100 (2016).
2. Schlumberger, M. J. & Torlantano, M. Papillary and follicular thyroid carcinoma. *Baillieres Best Pract Res Clin Endocrinol Metab.* **14**, 601–613 https://doi.org/10.1053/beem.2000.0105 (2000).
3. Ito, Y. *et al.* Overall Survival of Papillary Thyroid Carcinoma Patients: A Single-Institution Long-Term Follow-Up of 5897 Patients. *World J Surg.* **42**, 615–622 https://doi.org/10.1007/s00268-018-4479-z (2018).
4. Xing, M. BRAF mutation in thyroid cancer. *Endocr Relat Cancer.* **12**, 245–262 https://doi.org/10.1677/erc.1.0978 (2005).
5. Xing, M. *et al.* Association between BRAF V600E mutation and mortality in patients with papillary thyroid cancer. *Jama.* **309**, 1493–1501 https://doi.org/10.1001/jama.2013.3190 (2013).

6. Pak, K., Suh, S., Kim, S. J. & Kim, I. J. Prognostic value of genetic mutations in thyroid cancer: a meta-analysis. *Thyroid.* **25**, 63–70 https://doi.org/10.1089/thy.2014.0241 (2015).
7. Xing, M. *et al.* Association between BRAF V600E mutation and recurrence of papillary thyroid cancer. *J Clin Oncol.* **33**, 42–50 https://doi.org/10.1200/jco.2014.56.8253 (2015).
8. Ito, Y. *et al.* BRAF mutation in papillary thyroid carcinoma in a Japanese population: its lack of correlation with high-risk clinicopathological features and disease-free survival of patients. *Endocr J.* **56**, 89–97 https://doi.org/10.1507/endocrj.k08e-208 (2009).
9. Matsuse, M. *et al.* TERT promoter mutations and Ki-67 labeling index as a prognostic marker of papillary thyroid carcinomas: combination of two independent factors. *Sci Rep.* **7**, 41752 https://doi.org/10.1038/srep41752 (2017).
10. Landa, I. *et al.* Frequent somatic TERT promoter mutations in thyroid cancer: higher prevalence in advanced forms of the disease. *J Clin Endocrinol Metab.* **98**, E1562–1566 https://doi.org/10.1210/jc.2013-2383 (2013).
11. Liu, X. *et al.* Highly prevalent TERT promoter mutations in aggressive thyroid cancers. *Endocr Relat Cancer.* **20**, 603–610 https://doi.org/10.1530/erc-13-0210 (2013).
12. Alzahrani, A. S., Alsaadi, R., Murugan, A. K. & Sadiq, B. B. TERT Promoter Mutations in Thyroid Cancer. *Horm Cancer.* **7**, 165–177 https://doi.org/10.1007/s12672-016-0256-3 (2016).
13. Liu, T. *et al.* The age- and shorter telomere-dependent TERT promoter mutation in follicular thyroid cell-derived carcinomas. *Oncogene.* **33**, 4978–4984 https://doi.org/10.1038/onc.2013.446 (2014).
14. Liu, X. *et al.* TERT promoter mutations and their association with BRAF V600E mutation and aggressive clinicopathological characteristics of thyroid cancer. *J Clin Endocrinol Metab.* **99**, E1130–1136 https://doi.org/10.1210/jc.2013-4048 (2014).
15. Melo, M. *et al.* TERT promoter mutations are a major indicator of poor outcome in differentiated thyroid carcinomas. *J Clin Endocrinol Metab.* **99**, E754–765 https://doi.org/10.1210/jc.2013-3734 (2014).
16. Xing, M. *et al.* BRAF V600E and TERT promoter mutations cooperatively identify the most aggressive papillary thyroid cancer with highest recurrence. *J Clin Oncol.* **32**, 2718–2726 https://doi.org/10.1200/JCO.2014.55.5094 (2014).
17. Muzza, M. *et al.* Telomerase in differentiated thyroid cancer: promoter mutations, expression and localization. *Mol Cell Endocrinol.* **399**, 288–295 https://doi.org/10.1016/j.mce.2014.10.019 (2015).
18. Shi, X. *et al.* Association of TERT promoter mutation 1,295,228 C > T with BRAF V600E mutation, older patient age, and distant metastasis in anaplastic thyroid cancer. *J Clin Endocrinol Metab.* **100**, E632–637 https://doi.org/10.1210/jc.2014-3606 (2015).
19. Tanaka, A. *et al.* TERT mRNA Expression as a Novel Prognostic Marker in Papillary Thyroid Carcinomas. *Thyroid.* **29**, 1105–1114 https://doi.org/10.1089/thy.2018.0695 (2019).
20. Qasem, E. *et al.* TERT promoter mutations in thyroid cancer: a report from a Middle Eastern population. *Endocr Relat Cancer.* **22**, 901–908 https://doi.org/10.1530/ERC-15-0396 (2015).

21. Bullock, M. *et al.* TERT promoter mutations are a major indicator of recurrence and death due to papillary thyroid carcinomas. *Clin Endocrinol (Oxf).* **85**, 283–290 https://doi.org/10.1111/cen.12999 (2016).
22. Lee, S. E. *et al.* Prognostic Significance of TERT Promoter Mutations in Papillary Thyroid Carcinomas in a BRAF(V600E) Mutation-Prevalent Population. *Thyroid.* **26**, 901–910 https://doi.org/10.1089/thy.2015.0488 (2016).
23. Jin, L. *et al.* BRAF and TERT promoter mutations in the aggressiveness of papillary thyroid carcinoma: a study of 653 patients. *Oncotarget.* **7**, 18346–18355 https://doi.org/10.18632/oncotarget.7811 (2016).
24. Kim, T. H. *et al.* TERT promoter mutations and long-term survival in patients with thyroid cancer. *Endocr Relat Cancer.* **23**, 813–823 https://doi.org/10.1530/erc-16-0219 (2016).
25. Liu, R. *et al.* Mortality Risk Stratification by Combining BRAF V600E and TERT Promoter Mutations in Papillary Thyroid Cancer: Genetic Duet of BRAF and TERT Promoter Mutations in Thyroid Cancer Mortality. *JAMA Oncol.* **3**, 202–208 https://doi.org/10.1001/jamaoncol.2016.3288 (2017).
26. Giorgenon, T. M. V. *et al.* Preoperative detection of TERT promoter and BRAFV600E mutations in papillary thyroid carcinoma in high-risk thyroid nodules. *Arch Endocrinol Metab.* **63**, 107–112 https://doi.org/10.20945/2359-3997000000116 (2019).
27. Lorbeer, F. K. & Hockemeyer, D. TERT promoter mutations and telomeres during tumorigenesis. *Curr Opin Genet Dev.* **60**, 56–62 https://doi.org/10.1016/j.gde.2020.02.001 (2020).
28. Gerstung, M. *et al.* The evolutionary history of 2,658 cancers. *Nature.* **578**, 122–128 https://doi.org/10.1038/s41586-019-1907-7 (2020).
29. Landa, I. *et al.* Genomic and transcriptomic hallmarks of poorly differentiated and anaplastic thyroid cancers. *J Clin Invest.* **126**, 1052–1066 https://doi.org/10.1172/JCI85271 (2016).
30. Liu, R. & Xing, M. Diagnostic and prognostic TERT promoter mutations in thyroid fine-needle aspiration biopsy. *Endocr Relat Cancer.* **21**, 825–830 https://doi.org/10.1530/ERC-14-0359 (2014).
31. Nikiforov, Y. E. *et al.* Highly accurate diagnosis of cancer in thyroid nodules with follicular neoplasm/suspicious for a follicular neoplasm cytology by ThyroSeq v2 next-generation sequencing assay. *Cancer.* **120**, 3627–3634 https://doi.org/10.1002/cncr.29038 (2014).
32. Crescenzi, A. *et al.* Preoperative Assessment of TERT Promoter Mutation on Thyroid Core Needle Biopsies Supports Diagnosis of Malignancy and Addresses Surgical Strategy. *Horm Metab Res.* **48**, 157–162 https://doi.org/10.1055/s-0035-1548873 (2016).
33. Landis, J. R. & Koch, G. G. The measurement of observer agreement for categorical data. *Biometrics.* **33**, 159–174 (1977).
34. Ghossein, R. A., Katabi, N. & Fagin, J. A. Immunohistochemical detection of mutated BRAF V600E supports the clonal origin of BRAF-induced thyroid cancers along the spectrum of disease progression. *J Clin Endocrinol Metab.* **98**, E1414–1421 https://doi.org/10.1210/jc.2013-1408 (2013).
35. Correspondence Michiko Matsuse, PhD

36. Department of Radiation Medical Sciences,Atomic Bomb Disease Institute, Nagasaki University, Nagasaki, Japan.
37. -12-4 Sakamoto, Nagasaki 852–8523, Japan.
38. Tel +81-95-819-7116
39. Fax +81-95-819-7117
40. E-mail: michikom@nagasaki-u.ac.jp

Figures

Figure 1

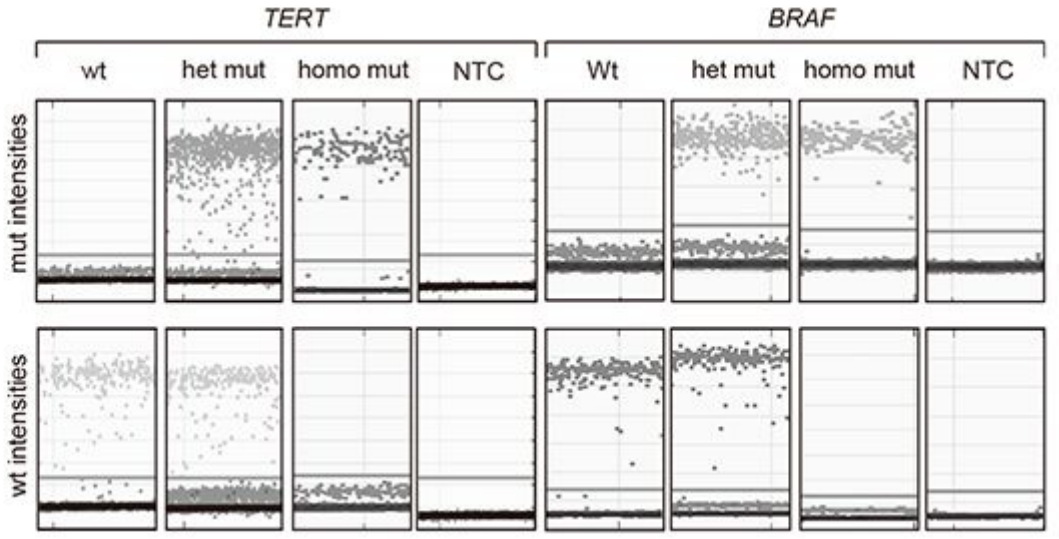

Figure 1

Specific detection of mutant and wild-type alleles of the TERT-p and BRAF by ddPCR. DNA of wild-type, heterozygous mutation (het mut), and homozygous mutation (homo mut) were analyzed by the ddPCR assay. Each dot represents a positive droplet of a mutant allele or a wild-type allele. NTC, no template control.

Figure 2

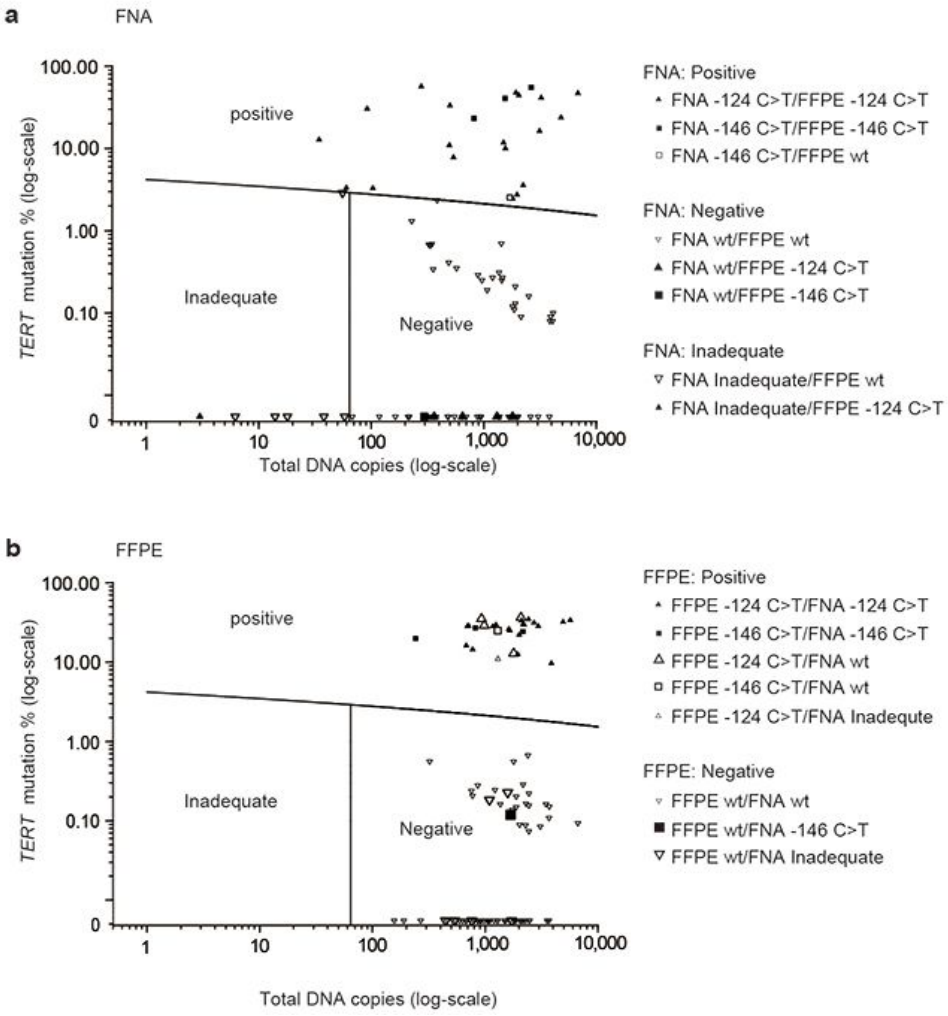

Figure 2

Detection of the TERT-p mutations in FNA and FFPE samples. The TERT-p mutational status was determined based on the number of total TERT-p DNA copy in a reaction (horizontal axis) and the percentage of the TERT-p mutation allele (vertical axis) using pre-established cutoff limits (Supplementary file 1). Each sample is represented by an open/closed triangle/square depending on the concordance with the corresponding counterpart. (a) FNA, (b) FFPE results.

Figure 3

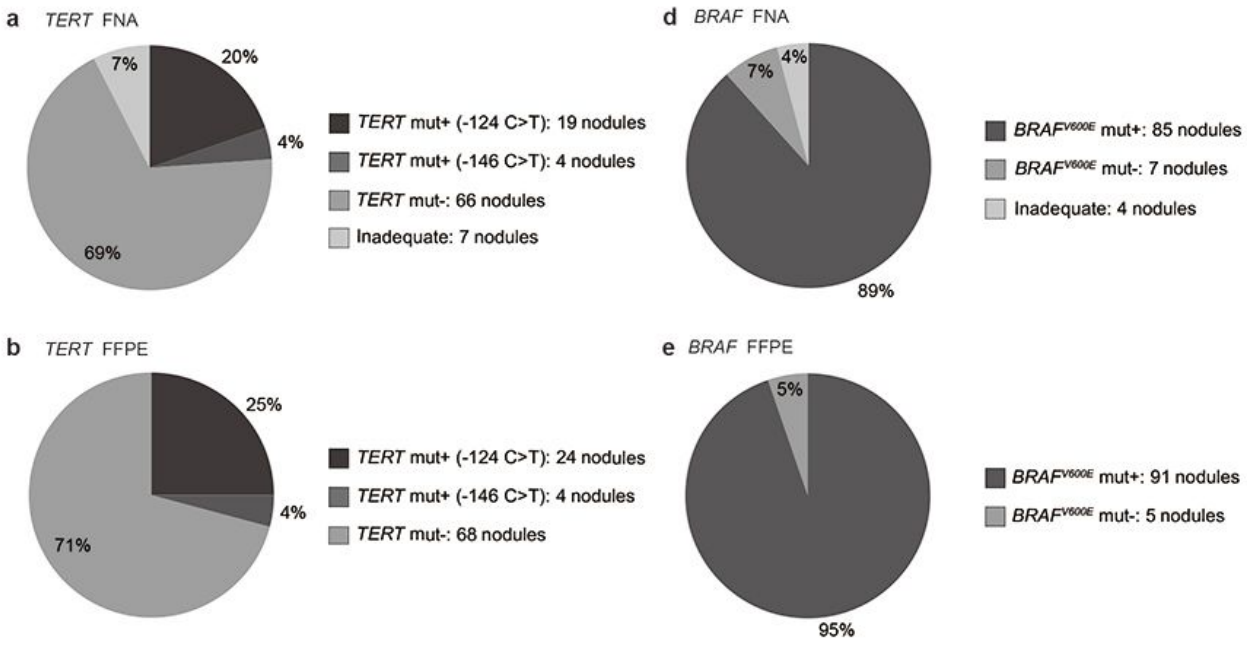

c

TERT status		On FNA	
		Positive	Negative
On FFPE	Positive	22	5
	Negative	1	61

Sensitivity: 22/(22+5)= 81.5%
Spesitivity: 61/(1+61)= 98.4%
Positive predictive value: 22/(22+1)= 95.7%
Negative predictive value: 61/(5+61)= 92.4%
Cohen's kappa: 0.834, p-value: 2.52×10^{-15}
AUC-ROC: 0.899 (95%CI: 0.810–0.989)

f

BRAFV600E status		On FNA	
		Positive	Negative
On FFPE	Positive	84	3
	Negative	1	4

Sensitivity: 84/(84+3)= 96.6%
Spesitivity: 4/(1+4)= 80.0%
Positive predictive value: 84/(84+1)= 98.8%
Negative predictive value: 4/(3+4)= 57.1%
Cohen's kappa: 0.710, p-value: 1.02×10^{-11}
AUC-ROC: 0.888 (95%CI: 0.679–1.000)

Figure 3

Summary of the TERT-p and the BRAFV600E mutations. (a) The pie chart of the TERT-p mutational status in the 96 FNA wash solutions. (b) The pie chart of the TERT-p mutational status in the 96 corresponding FFPE specimens. (c) The confusion matrix of the results of the TERT-p mutation detection in corresponding FNA and FFPE samples. (d) The pie chart of the BRAFV600E mutational status in the 96 FNA specimens. (e) The pie chart of the BRAFV600E mutational status in the 96 corresponding FFPE specimens. (f) The confusion matrix of the results of the BRAFV600E mutation detection in corresponding FNA and FFPE samples.

Figure 4

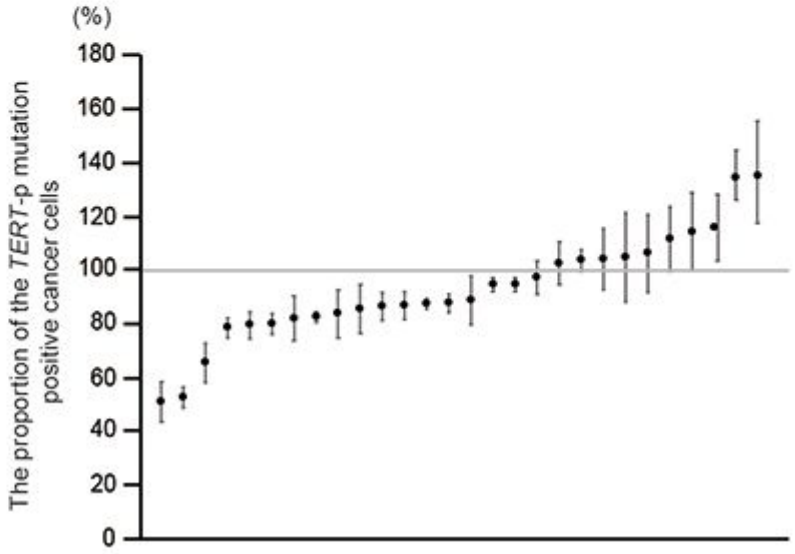

Figure 4

Clonality of the TERT-p mutation. The proportion of the TERT-p mutation-positive cancer cells (TP) was calculated in the 28 FFPE samples that were positive for the TERT-p mutation by dividing the allelic frequency of the TERT promoter mutation by the allelic frequency of the BRAFV600E mutation. In each case, the ddPCR was run in triplicates for both the TERT-p and BRAF. Each point represents the mean (filled circles) and standard deviation.

Supplementary Files

This is a list of supplementary files associated with this preprint. Click to download.

- NakaoSupplementaryfile.docx
- NakaoSupplementaryFigureLegends.docx
- SupplementaryFig.S1.ai
- SupplementaryFig.S2.ai
- SupplementaryFig.S3.ai